

# Saturation of the Xe III 109-nm laser using traveling-wave laser-produced-plasma excitation

M. H. Sher, J. J. Macklin, J. F. Young, and S. E. Harris

Edward L. Ginzton Laboratory, Stanford University, Stanford, California 94305

Received June 29, 1987; accepted August 14, 1987

We describe the construction and operation of a 109-nm, photoionization-pumped, single-pass laser in Xe III. The laser is pumped by soft x rays emitted from a laser-produced plasma in a traveling-wave geometry. Using a 3.5-J, 300-psec, 1064-nm laser pump pulse, we measure a small-signal gain coefficient of  $4.4 \text{ cm}^{-1}$  and a total small-signal gain of  $\exp(40)$ . The laser is fully saturated and produces an output energy of  $20 \mu\text{J}$  in a beam with 10-mrad divergence.

In this Letter we describe the construction and operation of a single-pass, 109-nm Xe III Auger laser.<sup>1</sup> The laser is pumped by soft x rays, which are emitted from a laser-produced plasma in a traveling-wave geometry. Using only 3.5 J of 1064-nm pump energy in a 300-psec pulse, we measure a small-signal gain coefficient of  $4.4 \text{ cm}^{-1}$  and a total small-signal gain of  $\exp(40)$ . The 109-nm laser is fully saturated over the second half of its length and produces an output energy of  $20 \mu\text{J}$  in a beam with 10-mrad divergence.

Population inversion of the 109-nm transition was proposed and demonstrated by Kapteyn *et al.*<sup>1,2</sup> The inversion mechanism, outlined in the energy-level diagram of Fig. 1, is inner-shell photoionization of a 4d electron, followed by Auger decay to Xe III. In this system, the Auger branching ratio is about 5% to both the upper and lower laser levels. The inversion results from the higher degeneracy of the lower level. Assuming only Doppler broadening, and ignoring hyperfine splitting, the gain cross section is  $3 \times 10^{-13} \text{ cm}^2$ .

Proposals for photoionization pumping of short-wavelength lasers and for Auger-pumped short-wavelength lasers were made by Duguay<sup>3</sup> and by McGuire.<sup>4</sup> The possibility of constructing such lasers at low pumping energies was delineated by the work of Caro *et al.*,<sup>5</sup> Silfvast *et al.*,<sup>6</sup> and Mendelsohn and Harris.<sup>7</sup> Recently Yin *et al.*<sup>8</sup> showed that small-signal gain coefficients within a factor of 2 of those reported here could be produced with several joules of pump energy and, in addition, that the Xe III 109-nm gain can be limited by competing processes. Their work suggests that the most efficient use of pump energy requires a long, high-aspect-ratio geometry.

Figure 2 is a schematic diagram of the traveling-wave laser-produced-plasma excitation source. A 1064-nm laser is incident upon a cylindrical lens at  $\theta = 68 \text{ deg}$  from normal and is focused onto a target that is parallel to the lens. This oblique focusing geometry has several advantages over the normal-incidence arrangements used in previous work.<sup>1,8</sup> The large angle of incidence expands the length of the line focus by  $1/\cos \theta$ ; therefore our 3.3-cm-diameter beam produces a

9-cm-long plasma. In addition, the pump laser sweeps across the target, and the leading edge of the plasma travels at a speed,  $c/\sin \theta$ , only 8% greater than that of light. The emitted soft x rays thus provide nearly synchronous traveling-wave excitation of the ambient gaseous medium.

In order to reduce the pump energy lost to grazing-incidence reflection, grooves were cut into the target surface at a 45-deg angle, as shown in the inset of Fig. 2. The grooved surface decreases the local angle of incidence of the *p*-polarized pump laser from 68 to 23 deg and divides the input beam to form many small, separated plasmas rather than one continuous line. The combined length of these plasmas is only slightly greater than the input beam diameter. As a result, the extended gain length can be pumped with increased 1064-nm intensity and improved soft-x-ray conversion efficiency.

All the experiments described here were performed with a 3.5-J, 300-psec FWHM pump laser with a repetition rate of 1 shot every 5 min. The 3.3-cm-diameter, spatially uniform input beam was compressed (using normal-incidence cylindrical optics) to 1.7 cm in the focusing dimension to increase the *f*-number of the

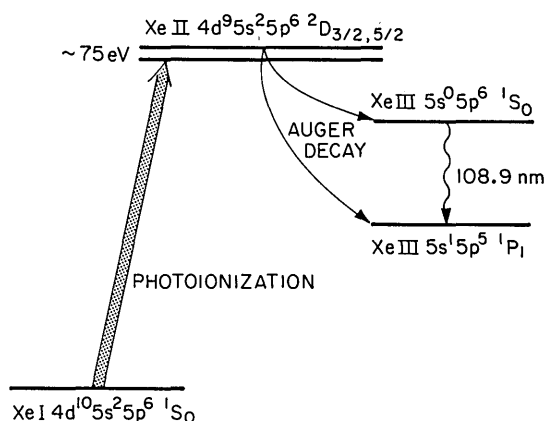


Fig. 1. Energy-level diagram of Xe showing the levels relevant to photoionization and to Auger pumping of Xe III.

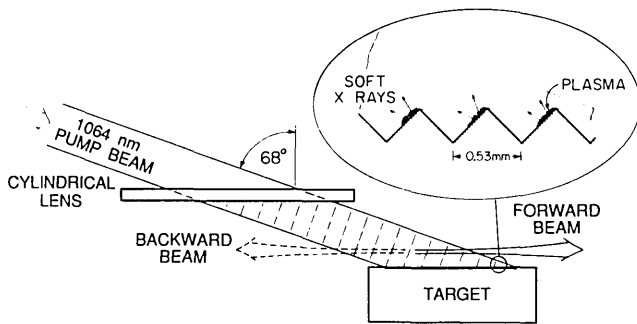


Fig. 2. Traveling-wave laser-produced-plasma soft-x-ray source.

lens and reduce aberrations. The focal length of the oblique cylindrical lens can be approximated by the sagittal focal length of a tilted spherical lens; for  $f_0 = 20$  cm and  $\theta = 68$  deg, the focal length is 12 cm. A 2.5-cm-diameter stainless-steel rod, threaded at 19 grooves  $\text{cm}^{-1}$  and electroplated with gold, served as the target. This arrangement produced a focal line width of  $200 \mu\text{m}$  and an intensity on target of about  $2 \times 10^{11} \text{ W cm}^{-2}$ . The ambient Xe pressure was 4 Torr.

The observed excited volume was defined by two plates separated by 1.5 mm, through which the 1064-nm pump laser was focused, and by two 2-mm-diameter pinholes on an axis 1.5 mm above the target and located 2 cm from the ends of the line focus. We monitored the 109-nm emission in the forward and backward directions simultaneously, using two 0.2-m VUV monochrometers coupled to windowless channel electron multipliers. A 1-mm-thick LiF window isolated each of the monochrometers from the Xe cell. To avoid saturation of the electron multipliers, we used calibrated LiF and  $\text{O}_2$  gas cell attenuators to achieve the  $10^5$  dynamic range required in these experiments.

The small-signal gain on the 109-nm transition was determined from measurements of time-integrated emission (the 109-nm pulses were shorter than the 700-psec response time of the detection system) as a function of length. The length of plasma on the target, and hence of the gain medium, was varied by masking the input laser beam. Figure 3 shows the increase in forward-propagating emission with length for three short sections of the target. A simple exponential fit to the data yields an average, time-integrated, small-signal gain coefficient of  $4.4 \text{ cm}^{-1}$ . This is a 70% improvement over the value obtained with a smooth, gold-plated target. Based on the measured, uniform small-signal gain coefficient, unsaturated amplification along the full 9 cm of length would provide a total gain of  $\exp(40)$ , or 170 dB.

The large-signal behavior of both the forward and backward 109-nm laser emission is shown in the semi-log and linear plots of Figs. 4(a) and 4(b), where each symbol represents the average of at least three data points. For short gain lengths, the slopes of the forward and backward energy versus length curves [on the log scale in Fig. 4(a)] are approximately the same. Beyond 4 cm of length, the forward beam grows linearly [Fig. 4(b)], while the backward emission remains

constant. This behavior indicates that the forward beam is fully saturated and is extracting nearly all the stored energy from the second half of the length.

The vertical scale of Fig. 4 was calibrated in units of energy by replacing the monochrometer-based detection systems with a fast (350-psec), calibrated vacuum photodiode ( $\text{Al}_2\text{O}_3$  photocathode) and a calibrated LiF window. The increase of energy with length was identical to that in the emission measurements made using

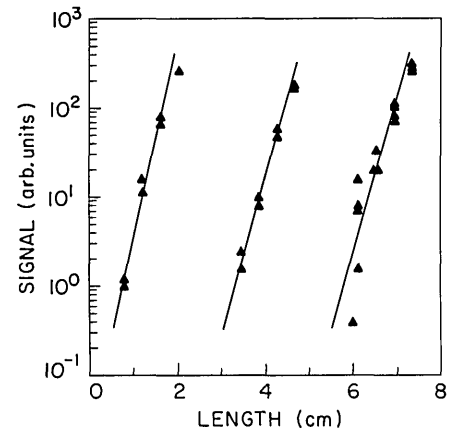


Fig. 3. 109-nm signal versus length for three different sections of the target. The average exponential gain coefficient is  $4.4 \text{ cm}^{-1}$ .

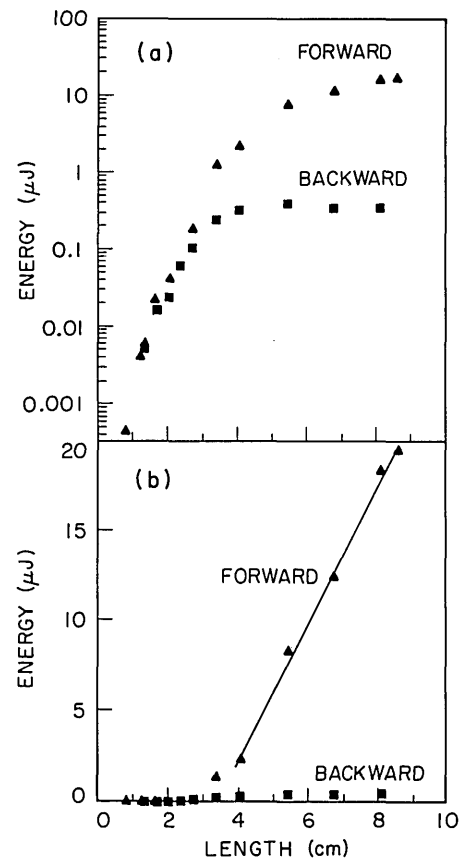


Fig. 4. 109-nm energy versus plasma length on (a) log scale, (b) linear scale showing saturated, linear growth of the forward beam.

the monochrometers. The maximum energy output was  $20 \mu\text{J}$  in the forward direction and  $0.4 \mu\text{J}$  in the backward direction, yielding a forward-to-backward emission ratio of 50:1.

By visual observation of fluorescence on a scintillator located 90 cm from the target, and by translation of the vacuum photodiode in this plane, we estimate a forward beam divergence of 10 mrad. This small divergence is consistent with the large aspect ratio (length/width  $\approx 60$ ) of the geometry. The pulse width of the 109-nm laser emission was less than the 350-psec time resolution of the photodiode, which implies an output power greater than 50 kW.

Assuming that the measured energy is extracted predominantly from the last 6 cm of gain length, the total energy stored in the observed volume is  $30 \mu\text{J}$ , or about  $10^{-5}$  of the 1064-nm pump energy. Taking the cross-sectional area of the laser to be  $0.03 \text{ cm}^2$ , we calculate an energy density of  $110 \mu\text{J cm}^{-3}$  stored in the 109-nm inversion. Given the atomic parameters of the system,<sup>2</sup> i.e., an average  $4d$  photoionization cross section of 15 Mb between 70 and 130 eV, the 5% Auger yield, and  $\sim 12\%$  quantum efficiency, we can deduce a conversion efficiency of 1064-nm light to useful soft x rays of approximately 2%.

The relationship of the observed gain behavior to the measured stored energy is complicated by the transient nature of the population inversion. The spontaneous lifetime of the upper level is 4.75 nsec,<sup>2</sup> but the inversion lifetime and the pulse length are governed by stimulated decay and are on a scale with the transit time of the gain medium. The large forward-to-backward emission ratio imparted by the traveling-wave excitation can be explained in terms of competition between the two beams. Although the slopes of the forward and backward energy-versus-length curves in Fig. 4(a) are similar for the shorter lengths, the forward beam reaches saturation earlier and, therefore, dominates in the second half of the length.

In this research we have demonstrated single-pass gain saturation of a photoionization-pumped laser.

We have employed a traveling-wave laser-produced-plasma geometry that efficiently excites an extended gain length using only a few joules of pump energy. These results represent a significant step in the development of practical photoionization-pumped lasers.

The authors thank G. Y. Yin for helpful discussions and H. N. Kornblum of Lawrence Livermore National Laboratory for the use of the vacuum photodiode. M. H. Sher gratefully acknowledges the support of an AT&T Ph.D. scholarship. J. J. Macklin gratefully acknowledges the support of an IBM Fellowship. This research was jointly supported by the U.S. Office of Naval Research, the U.S. Air Force Office of Scientific Research, the U.S. Army Research Office, the Strategic Defense Initiative Organization, and Lawrence Livermore National Laboratory.

*Note added in proof:* Recent streak-camera measurements indicate that the 109-nm pulse width is  $50 \pm 10$  psec FWHM, which implies a peak power of 0.4 MW.

## References

1. H. C. Kapteyn, R. W. Lee, and R. W. Falcone, *Phys. Rev. Lett.* **57**, 2939 (1986).
2. H. C. Kapteyn, M. M. Murnane, R. W. Falcone, G. Kolbe, and R. W. Lee, *Proc. Soc. Photo-Opt. Instrum. Eng.* **688**, 54 (1986).
3. M. A. Duguay, in *Laser Induced Fusion and X-Ray Laser Studies*, S. F. Jacobs, M. O. Scully, M. Sargent III, and C. D. Cantrell III, eds. (Addison-Wesley, Reading, Mass., 1976), p. 557.
4. E. J. McGuire, *Phys. Rev. Lett.* **35**, 844 (1975).
5. R. G. Caro, J. C. Wang, R. W. Falcone, J. F. Young, and S. E. Harris, *Appl. Phys. Lett.* **42**, 9 (1983).
6. W. T. Silfvast, J. J. Macklin, and O. R. Wood II, *Opt. Lett.* **8**, 551 (1983).
7. A. J. Mendelsohn and S. E. Harris, *Opt. Lett.* **10**, 128 (1985).
8. G.-Y. Yin, C. P. J. Barty, D. A. King, D. J. Walker, S. E. Harris, and J. F. Young, *Opt. Lett.* **12**, 331 (1987).